

Fast Decorrelating Monte Carlo Moves for Efficient Path Sampling

Enrico Riccardi, Oda Dahlen, and Titus S. van Erp*

Department of Chemistry, Norwegian University of Science and Technology, NO-7491 Trondheim, Norway

Many relevant processes in chemistry, physics, and biology are rare events from a computational perspective as they take place beyond the accessible time scale of molecular dynamics (MD). Examples are chemical reactions, nucleation, and conformational changes of biomolecules. Path sampling is an approach to break this time scale limit via a Monte Carlo (MC) sampling of MD trajectories. Still, many trajectories are needed for accurately predicting rate constants. To improve the speed of convergence, we propose two new MC moves, stone skipping and web throwing. In these moves, trajectories are constructed via a sequence of subpaths obeying super-detailed balance. By a reweighting procedure, almost all paths can be accepted. Whereas the generation of a single trajectory becomes more expensive, the reduced correlation results in a significant speedup. For a study on DNA denaturation the increase was found to be a factor 12.



Infrequent transitions between stable states are often not observable with straightforward molecular dynamics (MD). Several methods have been designed to sample the transitions, but most of them focus on statistics in configuration space (like the computation of free energy barriers¹) and approximate dynamical properties based on either transition state theory or Markovian assumptions.^{2,3} Path sampling⁴ is a completely different approach as it is directly focused on the dynamics of the process via an algorithm in which unbiased MD trajectories are sampled via a Monte Carlo (MC) scheme. The idea got very popular due to the transition path sampling method (TPS)⁵ which showed how this can be exploited for generating trajectories connecting the reactant and product states for a wide range of processes such as protein folding, nucleation, and chemical reactions.^{6,7} TPS also introduced a path sampling based algorithm for calculating rates though this approach was relatively expensive despite several improvements.⁸

In recent years, transition interface sampling (TIS)⁹ and its improvement replica exchange TIS (RETIS)¹⁰ have introduced an alternative rate calculation approach based on path sampling that is still exact, but considerably faster. The method fundamentally differs with TPS regarding both its theoretical framework and the algorithmic aspects. In TIS/RETIS, the rate of transition is calculated by combining the results of a series of path sampling simulations, each exploring a different path ensemble, defined by a set of non-intersecting interfaces $\{\lambda_0, \lambda_1, \dots, \lambda_N\}$ positioned along the progress coordinate. λ_0 and λ_N define the boundaries of reactant state *A* and product state *B*, respectively, while the remaining interfaces are positioned to maximize the efficiency of the sampling. The different TIS path ensembles $[i^+]$ for $i = 0, 1, \dots, N-1$ contain all paths, starting and ending at λ_0 , crossing λ_i at least once, and ending at λ_0 or λ_N . A detailed balance Monte Carlo (MC) approach for generating these trajectories ensures that the same distribution of paths are being generated as if the appropriate trajectories are cut out from an infinitely long MD trajectory.

RETIS¹⁰ improves the efficiency of TIS even further by employing replica exchange moves¹¹ between the path ensembles, but the principle MC move in any path sampling approach is still the so-called *shooting*⁵ move. In this MC step, a backward and forward in time integration from a slightly modified point of the previous path is performed. Many variations of this move have been suggested¹²⁻¹⁴ which mainly differ in the selection of the shooting point and its randomized modification. However, in all these variations, consecutive accepted paths share almost identical time slice(s) which is a severe source of correlations in the sampling.

In this Letter, we present highly efficient path-generating moves *Stone Skipping* (SS) and *Web Throwing* (WT), which decorrelate considerably faster by launching several subpaths in between full path generations (See Fig. 1). The SS move creates subpaths that bounce on the path ensemble's specific interface like a flat stone

thrown at the water surface. The WT move creates subpaths between two interfaces, creating a web. In addition, we improve the efficiency even more by introducing new path ensemble definitions in which the statistical weight of a path in ensemble $[i^+]$ depends on the number of λ_i interface crossings and on the end state of the path. This alternative path weight ensures that all trajectories are accepted except for trial trajectories hitting the reactant state in both time directions. The two moves are explained below.

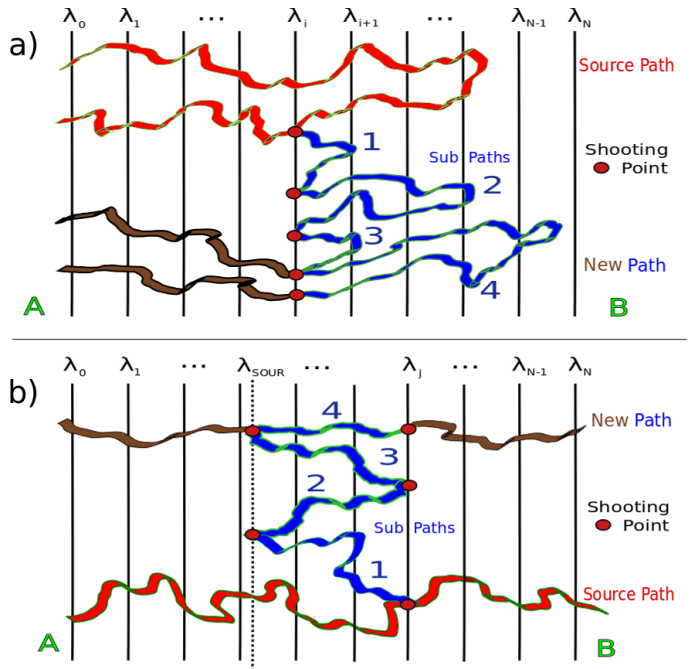


FIG. 1. Illustration of new MC moves for $N_s = 4$. a) Stone Skipping scheme for the $[i^+]$ ensemble. In red: source path, in blue: subpaths, in brown: path extensions for the last subpath. The shooting point represented by the red circles. From the source path a random point on the λ_i interface is selected and from this point subpaths 1-4 are generated. The last subpath 4 is finally completed and becomes the new full path. b) Web Throwing scheme for the $[j^+]$ ensemble. A random point at either λ_{SOUR} or λ_j is selected. Next, subpaths 1-4 connecting λ_{SOUR} or λ_j are generated and, finally, the last connecting path is extended in both time directions.

Stone Skipping. *Selection of the shooting point:* In the $[i^+]$ ensemble, for the creation of the first subpath *all* the crossings with λ_i of the old path (source path, see Fig. 1) has to be considered. For the next subpaths the *last* crossing of the latest subpath with λ_i must be considered. Each crossing is uniquely defined by a pair of consecutive points in phase-space, where the progress coordinate is either standing immediately before (a) or after (b) the interface λ_i . The new shooting point is randomly selected between the (a) and (b) points. *Generation of subpaths:* New random velocities are taken from a Maxwell-Boltzmann distribution for the selected shooting point. The velocities are accepted if a single in-

tegration step (forward or backward in time) produces a new crossing with λ_i . This velocity generation procedure is re-iterated until this condition is met. Using the first accepted velocities, a new subpath is generated starting at the λ_i interface (Blue line segment 1 in Fig. 1a) and ending at either state B , or interface λ_i . If the new subpath ends at λ_i , the last 2 frames of the paths eventually constitutes the new (a) and (b) shooting points for the next subpath. If the subpath reaches state B , its first (a),(b) crossing points are to be considered. This process is re-iterated for the number of desired subpaths for each cycle. *Generation of a new path*: First the physical time-direction along the last subpath is chosen at random. Then, the last subpath is propagated backward and forward in time. If the backward integration ends in A , the new full path will be accepted or rejected depending on the number of crossings with λ_i (See below). The new path is therefore composed by the last generated subpath (blue subpath 4 in Fig. 1a) and its extension (in brown).

Web Throwing. A new interface λ_{SOUR} (surface of unlikely return) has to be defined along the progress coordinate. It is chosen at the reactant side of the free energy barrier such that if it is crossed towards the direction of the reactant state, the path will most likely end up in state A . *Selection of the shooting point.* The segments of the previous path going from λ_{SOUR} to λ_j along the forward time-direction have to be selected first (in the red source path in Fig. 1b, only one of such segments is present). Each segment has four points that define the crossings of the source path with λ_{SOUR} and λ_j . Here, we will focus on WT for stochastic dynamics without momenta-change for which only the two interior points are considered and the new shooting point is randomly selected between these. In the SI, we briefly discuss some variations of the WT move. *Generation of subpaths*: A new subpath is generated keeping the same positions and velocities of the selected shooting point. Depending on the originating interface, the equations of motion are either integrated backward or forward in time (in Fig. 1b, subpath 1 and 3 are propagated backward in time, subpath 2 and 4 are propagated forward in time). If the new subpath connects both interfaces λ_j and λ_{SOUR} , the new subpath is considered for selecting the new shooting points. Otherwise, a new shooting point is randomly selected again from the previous segment. In either case, each failed or successful subpath has to be accounted, and the procedure is repeated for the number of desired subpaths for each cycle. *Generation of a new path*: The last generated subpath connecting λ_{SOUR} to λ_j is propagated backward and forward in time until reaching λ_0 or λ_N generating a new full path. If the path starts at λ_0 it can be accepted (or rejected) based on the number of λ_{SOUR} to λ_j connecting segments.

As shown in the Supplementary Information (SI), the generation of completed paths in SS and WT fulfills super-detailed balance, which is commonly used for designing efficient MC moves for the study of polymer

adsorption in porous media (configurational bias MC (CBMC)¹⁵). Here, we use the same type of procedure where trajectories grow from subpaths, instead of polymers from atoms, based on the following generic acceptance probability

$$P_{\text{acc}} = \min \left[1, \frac{P(p^{(n)})P_{\text{gen}}(p^{(n)} \rightarrow p^{(o)} \text{ via } \bar{\chi})}{P(p^{(o)})P_{\text{gen}}(p^{(o)} \rightarrow p^{(n)} \text{ via } \chi)} \right] \quad (1)$$

where $P(p^{(o)})$ and $P(p^{(n)})$ are the probabilities of the old and new path, respectively, and $P_{\text{gen}}(p \rightarrow p' \text{ via } \chi)$ and $P_{\text{gen}}(p \rightarrow p' \text{ via } \bar{\chi})$ are the probabilities to generate path p' from path p using a specific construction path χ and its unique inverse construction path $\bar{\chi}$. As shown in the SI, this leads to rather simple acceptance rules for both SS and WT

$$\text{SS} : P_{\text{acc}} = \min \left[1, \frac{n_c^{(o)}}{n_c^{(n)}} \right], \text{WT} : P_{\text{acc}} = \min \left[1, \frac{n_s^{(o)}}{n_s^{(n)}} \right] \quad (2)$$

where $n_c^{(o)}$, $n_c^{(n)}$ are the number of crossings with λ_i and $n_s^{(o)}$, $n_s^{(n)}$ are the number of selectable $\lambda_{\text{SOUR}}-\lambda_j$ segments of the old and new path, respectively. In addition, the new path needs to fulfill the path ensemble's specific condition (starting at λ_0 and crossing λ_i at least once).

There are essential differences between the application of super-detailed balance in CBMC and the application of this concept in this Letter. CBMC is based on growing tree-like structures in which branches are selected for further growth based on Rosenbluth factors.¹⁶ Using this idea in path sampling has been suggested by one of us,¹⁷ but the range of systems for which this approach is useful is limited (e.g. it cannot be applied to deterministic dynamics). The interpretation of super-detailed balance that we give via construction paths and inverse construction paths is more general and opens up very different ways to exploit the concept like we do in this Letter. Also, so-far the use of super-detailed balance has only been invoked for cases where the acceptance of the normal Monte Carlo move is extremely low. That is not the case here where the standard shooting move gives decent acceptance ($\sim 30 - 50\%$). The use of super-detailed balance to speed-up the decorrelation of the sampling is new. Therefore, we think that our approach might lead to other algorithmic applications outside the path sampling methodology.

The generation of several subpaths for each new path generation makes the MC moves more expensive than simple shooting. However, it takes several shooting moves, determined by the statistical inefficiency \mathcal{N} of the sampling, before a really new uncorrelated path is generated. Paths in between can be viewed as near-duplicates and do not lower the statistical accuracy. By the generation of $N_s < \mathcal{N}$ subpaths with average length l_s one reduces the statistical inefficiency between the full paths with average length l_p by approximately a factor $1/N_s$. Since the computational cost for obtaining a predefined error is proportional to the cost of an MC step and the statistical inefficiency, one can expect a relative increase

in efficiency by $l_p/N_s^{-1}(l_p + (N_s - 1)l_s)$. For large N_s this simplifies to l_p/l_s . Hence, the method of this Letter will especially be efficient for largely correlated sampling (large \mathcal{N}) and when $l_p \gg l_s$. The cost of the RETIS simulation using the new MC moves can then be comparable to that of approximate path sampling methods like partial path TIS² and milestoneing.³

Rejections, however, would imply that all N_s generated subpaths are wasted as one has to start from the previous full l_p path. It is therefore important to maximize the acceptance, which we achieved by modifying the path ensemble definition. First, if the last subpath completed backward in time ends up in state B , it is not directly rejected. Instead, the forward in time integration is performed and if that time direction ends in A , the path is accepted after a time-reversal operation on the path. Second, the weight of the path p in ensemble $[i^+]$ is adjusted by a factor w_i

$$\tilde{P}(p) = w_i(p)P(p) \equiv n_{c,i}(p)q(p)P(p) \text{ for } p \in [i^+] \quad (3)$$

where $P(p)$ is the original TPS weight for the path, $n_{c,i}(p)$ is the number of crossings with interface i , and $q(p)$ equals 2 for $A \rightarrow B$ and 1 for $A \rightarrow A$ paths. Using these new path weights, the acceptance probability of Eq. 2 becomes 1 (see SI), i.e. rejections only occurs if the path ends up in state B along both time directions. By reweighting each path by $w_i(p)^{-1}$, one reobtains all the correct statistics as with the original path weight $P(p)$ instead of $\tilde{P}(p)$. Since the new weight depends on the number of crossings with interface λ_i , the replica exchange moves have to be adjusted, as show in the SI.

To test the efficiency of the proposed method, we first consider a particle in a two-dimensional potential

$$V(x, y) = (x^2 + y^2)^2 - 10e^{-30(x-0.2)^2 - 3(y-0.4)^2} - 10e^{-30(x+0.2)^2 - 3(y+0.4)^2} \quad (4)$$

The potential has two minima and a saddle point (see Fig. 2). Reduced units are used such that the particle's mass and Boltzmann constant are equal to one: ($k_B = m = 1$). Visually, it is apparent that a good progress coordinate would be a function of both x and y and a linear combination would be sufficient for an efficient sampling using standard rare event free energy methods. However, since the selection of a good progress coordinate is most often not accessible nor intuitive in complex systems, we examined two non-ideal progress coordinates: x and y . The x coordinate requires a significant diffusion along the orthogonal direction, while the y coordinate has two minima separated by a barrier in the orthogonal direction at its maximum $y = 0$, a characteristic that causes troublesome hysteresis in free energy methods. Hysteresis is less affecting the efficiency of TIS/RETIS,¹⁸ but still represents a significant challenge.

Considering x and y as progress coordinate, we defined 7 and 8 interfaces, respectively (see Fig. 2). Furthermore, to ensure the stability of the states A and B , we applied

an additional condition that the potential energy must be lower than -9.0 to be considered in the stable states.

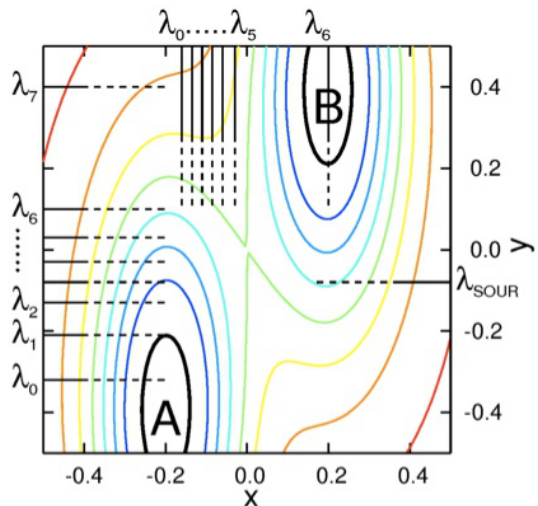


FIG. 2. Contour plot of the 2D potential. Thin isopotential lines differ by $3k_B T$. Thick black isopotential lines show the $V = -9$ stable state definitions. Interfaces for both x and y (including λ_{SOUR}) are shown at the edges.

A Langevin thermostat with friction coefficient $\gamma = 0.3$ controlled the temperature at $T = 0.4$. The time step was $dt = 0.003$. Furthermore, a 12.5% probability has been selected for the standard shooting move or for the new MC moves, 12.5% for a time-reversal, and a 75% for a replica exchange move. In the simulations performed considering the order parameter x , only SS has been applied, while the ones along y , SS has been applied in all ensembles except the last where the hysteresis is strongest. Here WT has been selected with $\lambda_{\text{SOUR}} = -0.13$. In total, we performed $200 \cdot 10^6$ and $120 \cdot 10^6$ MC cycles for RETIS using standard shooting and SS, respectively, for the x order parameter case. One MC cycle implied an update of all path ensembles a by a single MC step. For the y as order parameter case, $200 \cdot 10^6$ and $160 \cdot 10^6$ MC cycles were performed using standard shooting and SS/WT, respectively. These are considerably more cycles than one would normally perform, but it is necessary to obtain an accurate and reliable quantification of the statistical errors.

In the SI, a plot of the correlation and the computational cost per cycle as a function of N_s is reported for the last ensembles $[(N - 1)^+]$. It shows that the optimum efficiency is reached for $N_s \approx 4$ or 8 subpaths. For more complex systems, which tend to show more correlations in the sampling, a larger N_s is expected to be optimal. Therefore, we used $N_s = 4$ for the 2D system and $N_s = 8$ for a more complex system that is discussed later on. Further optimization is likely obtained by varying the N_s values for different path ensembles.

Fig. 3a shows rate constant as a function of the number of force evaluations for the 2D system using the x -

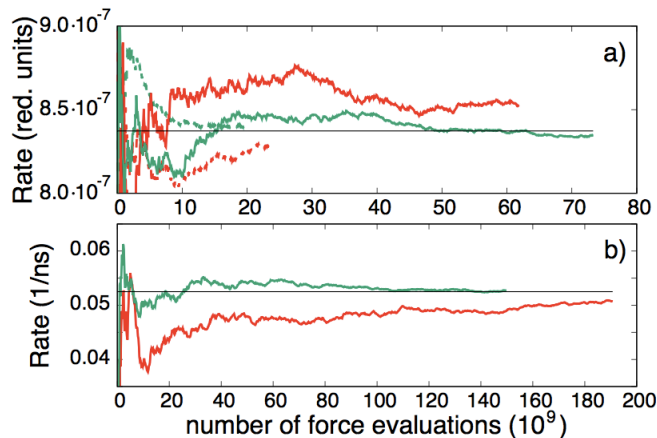


FIG. 3. Rate constant as function of the force evaluations calculated from RETIS simulations with standard shooting (red) and with new MC moves (green). a) results for the 2D potential with the progress coordinate along the x -axis (dashed) and y -axis (solid). The horizontal line is the average of the new MC results along x and y . b) Results for the mesoscopic DNA denaturation model. The horizontal line is the nearly exact result using the iterative integration method.¹⁰

and y -coordinate. Clearly, for both x and y the new MC scheme converges faster to a nearly similar value. The results of Fig. 3 can also be converted into blocks which, if large enough, can be viewed as independent full rate evaluations. Based on a division into eight blocks, we evaluated the improvement of efficiency to be a factor 4.7 along the x - and a factor 2.2 along the y -direction. In order to sample the hysteresis region (last ensemble along y), the WT move was essential. SS poorly samples in the last region since a lot of paths and subpaths connect to state B implying that the next shooting point is almost identical to the previous one. Hence, the SS moves seem to be the most efficient whenever the path ensemble explores the purely increasing part of the free energy barrier, but once a large fraction of the trajectories ends up in the product state, WT moves need to be invoked.

In high-dimensional complex systems, where the explorations in the orthogonal directions are critical, we expect that the relative efficiency will be even larger. To test this hypothesis, we repeated the calculations of Ref. 10 on DNA denaturation of a 20 AT basepair chain using the mesoscopic Peyrard-Bishop-Dauxois (PBD) model.¹⁹ All parameters are the same as the ones of Ref. 10, but simulations were performed considerably longer ($27 \cdot 10^6$ cycles for standard shooting and $15 \cdot 10^6$ for SS) and the number of interfaces was reduced from 8 to 7 by removing the λ_{N-1} interface. This reduces the number of $B \rightarrow B$ paths in the last ensemble which is advantageous for the new MC scheme, while it produces nearly the same efficiency for the standard shooting. In the new MC method only SS was applied with $N_s = 8$.

An excellent feature of the PBD model is that it has sufficient complexity to be used as a challenging test for MD based methods, but still has only first-neighbor interactions which allows us to integrate out the partition function using the iterative integration method with several digits precision.¹⁰ In addition, the dedicated approach of Ref. 10 allows the efficient computation of the transmission coefficient for the PBD model even at very low values. Using the combination of these two approaches as in Ref. 10, but with ten times more transmission cycles (40 million), we re-obtained a very similar rate constant ($5.25 \cdot 10^{-2}$ vs $5.24 \cdot 10^{-2} \text{ ns}^{-1}$ previously). This value can thus be viewed as a nearly exact independent reference.

Fig. 3b reports the computed rate constant versus the number of force evaluations for both standard shooting and SS. The latter converged very closely to the reference value ($5.27 \cdot 10^{-2} \text{ ns}^{-1}$) while the standard shooting is further off despite significantly more force iterations ($5.07 \cdot 10^{-2} \text{ ns}^{-1}$). Based on the block averages, we obtained relative errors of 1.1 and 3.5% respectively. The relative efficiency is obtained by the ratio between the squared error times the total number of force evaluations of the two simulation, resulting in a factor 12.3 faster for the SS approach. This value is, however, very sensitive to the number of blocks used in the analysis. Yet, since the absolute deviation from the reference value is 3.4% and 0.4% for shooting and SS, respectively, an order of magnitude improvement seems a rather conservative estimate. Furthermore, the new sampling method is considerably more memory effective since it requires fewer operations such as copying memory intensive double precision vectors. This effect is not considered in our efficiency analysis based on the number of force evaluations. Using the alternative path definition, the acceptance of the SS moves was 95% in the last ensemble and more than 99% in all others.

The statistical inefficiency \mathcal{N} and the path ratio's l_p/l_s determine how much faster the new MC moves are relatively to standard shooting. The SI shows these two values as function of the number of base pairs in the PBD model. \mathcal{N} increases, but l_p/l_s has not a clear trend and fluctuates between 15 and 20. However, if l_p/l_s ratio is large, the relative speed-up will increase with increasing complexity (until reaching a limiting value $\approx l_p/l_s$).

To conclude, we developed effective MC moves for path sampling based on super-detailed balance. Since the sampling utilizes short subpaths the cost becomes comparable to methods relying on Markovian approximations. Especially in the field of rare event Ab Initio MD simulations,²⁰ this is an important step forward. Since transition durations are typically only a few picoseconds, Markov State models (MSM)²¹ are generally not applicable. In addition, in biological systems where MSM has been very successful, strengths of different approaches can be combined. The multiple state TIS²² has already created a bridge between RETIS and the MSM methods and the new MC path moves can straightforwardly be

implemented in such an approach.

Supportive Information

The Supportive Information is available free of charge on the ACS website at DOI: xxx

Mathematical proof of the super-detailed balance relation and the high-acceptance approach, discussion on algorithmic variations, figures related to efficiency, pa-

rameter optimization, and scaling behavior.

Acknowledgements

We would like to thank Anders Lervik for carefully reading this paper and the Research Council of Norway for funding (project number 237423)

*titus.van.erp@ntnu.no

-
- ¹ Laio, A.; Parrinello, M. Escaping free-energy minima. *Proc. Natl. Acad. Sci. USA* **2002**, *99*, 12562.
- ² Moroni, D.; Bolhuis, P. G.; van Erp, T. S. Rate constants for diffusive processes by partial path sampling. *J. Chem. Phys.* **2004**, *120*, 4055–4065.
- ³ Faradjian, A. K.; Elber, R. Computing time scales from reaction coordinates by milestoning. *J. Chem. Phys.* **2004**, *120*, 10880.
- ⁴ Pratt, L. R. A Statistical Method for Identifying Transition-States in High Dimensional Problems. *J. Chem. Phys.* **1986**, *85*, 5045.
- ⁵ Dellago, C.; Bolhuis, P. G.; Chandler, D. Efficient transition path sampling: Application to Lennard-Jones cluster rearrangements. *J. Chem. Phys.* **1998**, *108*, 9236.
- ⁶ Bolhuis, P. G.; Chandler, D.; Dellago, C.; Geissler, P. Transition path sampling: Throwing ropes over rough mountain passes, in the dark. *Annu. Rev. Phys. Chem.* **2002**, *53*, 291–318.
- ⁷ Dellago, C.; Bolhuis, P. G.; Geissler, P. L. Transition path sampling. *Adv. Chem. Phys.* **2002**, *123*, 1–78.
- ⁸ Dellago, C.; Bolhuis, P. G.; Chandler, D. On the calculation of reaction rate constants in the transition path ensemble. *J. Chem. Phys.* **1999**, *110*, 6617.
- ⁹ van Erp, T. S.; Moroni, D.; Bolhuis, P. G. A Novel Path Sampling Method for the Sampling of Rate Constants. *J. Chem. Phys.* **2003**, *118*, 7762–7774.
- ¹⁰ van Erp, T. S. Reaction rate calculation by parallel path swapping. *Phys. Rev. Lett.* **2007**, *98*, 268301.
- ¹¹ Swendsen, R. H.; Wang, J. S. Replica Monte-Carlo Simulation of Spin-Glasses. *Phys. Rev. Lett.* **1986**, *57*, 2607–2609.
- ¹² Gruenwald, M.; Dellago, C.; Geissler, P. L. Precision shooting: Sampling long transition pathways. *J. Chem. Phys.* **2008**, *129*, 194101.
- ¹³ Mullen, R. G.; Shea, J.-E.; Peters, B. Easy Transition Path Sampling Methods: Flexible-Length Aimless Shooting and Permutation Shooting. *J. Chem. Theory Comput.* **2015**, *11*, 2421–2428.
- ¹⁴ Rowley, C. N.; Woo, T. K. New shooting algorithms for transition path sampling: Centering moves and varied-perturbation sizes for improved sampling. *J. Chem. Phys.* **2009**, *131*, 234102.
- ¹⁵ Frenkel, D.; Smit, B. *Understanding molecular simulation*, 2nd ed.; Academic Press: San Diego, CA, 2002.
- ¹⁶ Smit, B.; Siepmann, J. I. Computer Simulations of the Energetics and Siting of *n*-Alkanes in Zeolites. *J. Phys. Chem.* **1994**, *98*, 8442–8452.
- ¹⁷ van Erp, T. S.; Bolhuis, P. G. Elaborating Transition Interface Sampling Methods. *J. Comput. Phys.* **2005**, *205*, 157–181.
- ¹⁸ van Erp, T. S. Efficiency analysis of reaction rate calculation methods using analytical models I: The two-dimensional sharp barrier. *J. Chem. Phys.* **2006**, *125*, 174106.
- ¹⁹ Dauxois, T.; Peyrard, M.; Bishop, A. R. Entropy-driven DNA denaturation. *Phys. Rev. E* **1993**, *47*, R44–R47.
- ²⁰ Moqadam, M.; Riccardi, E.; Trinh, T. T.; Lervik, A.; van Erp, T. S. Rare event simulations reveal subtle key steps in aqueous silicate condensation. *Phys. Chem. Chem. Phys.* **2017**, *19*, 13361–13371.
- ²¹ Chodera, J. D.; Singhal, N.; Pande, V. S.; Dill, K. A.; Swope, W. C. Automatic discovery of metastable states for the construction of Markov models of macromolecular conformational dynamics. *J. Chem. Phys.* **2007**, *126*, 155101.
- ²² Du, W.-N.; Bolhuis, P. G. Adaptive single replica multiple state transition interface sampling. *J. Chem. Phys.* **2013**, *139*, 044105.